acta physica slovaca vol. 49 No. 3, 419 – 428 **June 1999**

ELECTRICAL RESPONSE OF DOPED YTTRIA STABILIZED ZIRCONIA

M. Hartmanová[†1], F. Kundracik[‡], J. Schneider[¶], T.V. Oreshnikova[$]
[†] *Institute of Physics, Slovak Acad.Sci., 84228 Bratislava, Slovakia*
[‡] *Department of Physics, Faculty of Mathematics and Physics, Comenius University, 84215 Bratislava, Slovakia*
[¶] *Institute of Crystallography and Mineralogy, University of Munich, 8000 Munich 2, Germany*
[$] *Institute of Crystallography, Russian Acad.Sci., 117333 Moscow, Russia*

Received 8 February 1999, accepted 4 April 1999

Electrical conductivity and the electrical response of undoped yttria stabilized zirconia (YSZ) as well as the influence of dopant addition (Fe_2O_3, Nb_2O_3 and CuO) on the oxygen sublattice were investigated. The results obtained are discussed and compared by means of various mechanisms of electrical response (impedance/admittance, relative permittivity / electrical modulus). The proposed substitutional model of solid solutions for all investigated systems is in a good agreement with the measured characteristics.

PACS: 61.10.Nz, 61.72.Ji, 72.20.Jv, 72.80.Sk, 77.84.Bw, 81.05.Jl, 84.37.+q

1 Introduction

Stabilized zirconia is at present one of the most important and widely used high-temperature materials. ZrO_2 fully stabilized with Y_2O_3 is of considerable interest as the solid oxide electrolyte that exhibits a high ionic conductivity. The number of applications continues to grow with the fast evolution of technology.

The variable-frequency methods are used almost exclusively in the area of ionic conduction in solids. The electrical frequency-response measurements (the measurements of the small-signal frequency response) are usually carried out at the impedance or complex-dielectric-constant - level [1]. The temperature dependence of the relevant resistances and permittivities is possible to determine from such measurements. The electrical *ac* data may be presented in any of four interrelated complex plane formalisms [2] :

- Impedance Z^*
- Admittance $Y^* = 1/Z^*$
- Relative permittivity $\varepsilon_r^* = 1/(j\omega C_0 Z^*)$
- Electric modulus $M^* = 1/\varepsilon_r^* = j\omega C_0 Z^*$

[1] E-mail address: fyzihart@savba.sk

Sample x. wt. % M_2O_3 (resp. MO)	Lattice parameter a_0 [nm]	Ionic radius r [nm]
0	0.51510(2)	R(Zr^{4+})=0.084 r(Y^{3+}) =0.1015 r(O^{2-}) = 0.142
0.1 Nb_2O_3	0.515368	r(Nb^{3+})=0.070
0.3 Fe_2O_3	0.514640	r(Fe^{3+}) = 0.078
2.0 CuO	0.516790	R(Cu^{2+}) = 0.073

Table 1. The estimated lattice parameters of Zr_2 + 12 mol % Y_2O_3 + x. wt. % M_2O_3 (resp. MO) and the ionic radii according to Shannon [6].

where $j = \sqrt{-1}$, ω is the angular frequency $2\pi f$ and $C_0 = \varepsilon_0 A/l$ in which C_0 is the geometrical capacitance of the cell with the dielectric medium being replaced by free space (vacuum), ε_0 is the permittivity of free space, 8.854×10^{-14} F cm^{-1}, l and A are the thickness and area of the sample. Analysis of such data provides the insight into the detailed microscopic, processes present in the full electrode and bulk material system.

The purpose of the present work is to investigate the electrical conductivity and electrical response of undoped yttria stabilized zirconia (YSZ) as well as the influence of dopant addition (Fe, Nb and Cu) on the oxygen sublattice of YSZ. The utilization of various mechanisms of electrical response mentioned above (impedance/admittance, relative permittivity / electrical modulus) allows to compare the results obtained.

2 Experimental

Preparation of samples: ZrO_2 + 12 mol% Y_2O_3 (YSZ) doped with 2 wt.% CuO, 0.3 wt.% Fe_2O_3 and 0.1 wt.% Nb_2O_3 were prepared as single crystals by a cold crucible directional solidification process known as a skull technique [3]. The ceramic form of undoped YSZ was prepared by the method described in [4].

Lattice parameter: the single crystals were milled into the powder and analyzed using X-ray diffraction (XRD) to determine the crystallographic phase and the lattice parameter. The determination was performed by means of STOE CIE GmbH powder diffractometer using $CuK_{\alpha 1}$ radiation and high purity lanthanum hexaborite (LaB_6) as an X-ray powder diffraction line position and profile shape standard. Tungsten was used as an internal standard [5].

ac conductivity measurements: were performed by an impedance technique in air. A Solartron SI 1260 impedance / gain phase analyzer interfaced to computer and run through a Labview program was used.The impedance measurements were made in the frequency range 10 Hz - 1 MHz and at temperatures 180^o - 560^{o}C. The temperature was stabilized by Chinoterm 10A digital temperature controller with the accuracy of $\pm 0.5^o$C. Platinum paste electrodes were applied to the entire faces of the sample.

3 Results and discussion

3.1 Lattice parameter and defect structure

The lower valent oxides such as CuO, Fe_2O_3 and Nb_2O_3 can disolve in YSZ, as clearly indicated by our X-ray data (Table 1). All investigated systems exhibit *fcc* fluorite structure with the observed slight change of lattice parameter a_0 of YSZ in dependence on the addition of dopants (Table 1). No additional phases were indentified in the powder diffraction patterns.

The knowledge of various types of lattice defects, the concentration and mobility of which are important parameters, is essential to explain the conductivity behaviour. When Y_2O_3 is added into ZrO_2, Y^{3+} ions substitute to the lattice sites of Zr^{4+} ions creating the oxygen vacancies $V_O^{\cdot\cdot}$ (in accordance with the Kroger-Vink notation). The reaction can be written as

$$\mathrm{Y_2O_3} \rightarrow 2\mathrm{Y}'_{\mathrm{Zr}} + V_{\mathrm{O}}^{\cdot\cdot} + 3\mathrm{O_O}. \tag{1}$$

The foreign metal ions should be smaller or comparable in size to the ionic radius of Zr^{4+}. This is clearly obeyed for Cu^{2+} as well as for Fe^{3+} and Nb^{3+} (Table 1.). When M_2O_3 resp. MO is added into YSZ, M^{3+} resp. M^{2+} ions can choose a zirconium ion site (substitutional doping) or an interstitial site. In the case of substitution, it forms an oxygen vacancy as follows:

$$\mathrm{MO} \rightarrow \mathrm{M}''_{\mathrm{Zr}} + V_{\mathrm{O}}^{\cdot\cdot} + \mathrm{O_O} \tag{2}$$

$$\mathrm{M_2O_3} \rightarrow 2\mathrm{M}'_{\mathrm{Zr}} + V_{\mathrm{O}}^{\cdot\cdot} + 3\mathrm{O_O} \tag{3}$$

and in the case of interstitial solid solution

$$\mathrm{MO} + \mathrm{V_O} \rightarrow 2\mathrm{M}''_i + \mathrm{O_O} \tag{4}$$

$$\mathrm{M_2O_3} + 3\mathrm{V}_{\mathrm{O}}^{\cdot\cdot} \rightarrow 2\mathrm{M}'''_i + 3\mathrm{O_O} \tag{5}$$

Substitutional model: the introduction of substitutional ions of small radii as in reactions (2) and (3), will probably have little effect on the lattice parameter, which is largely determined by the larger oxygen ions.

Interstitial model : the formation of interstitial ions as in reactions (4) and (5) will give rise to expansion of the lattice; however, the removal of oxygen vacancies will have the opposite effect. If our observations and arguments are correct, then we can assume that the substitutional doping takes place.

3.2 Electrical conductivity : Correlation with the structural model

ac - impedance technique has been demonstrated to be a powerful tool for the characterization of solid electrolytes, such as YSZ (e.g.[7,8]). The bulk, grain boundary and electrode processes can be often separated in a single experiment. In the present work, this technique was used to determine the electrical conductivity and the related electrical characteristics as a function of the temperature for the cells:

$$(-)\mathrm{air, Pt/YSZ, +Nb_2O_3, +Fe_2O_3, +CuO/Pt, air}(+). \tag{6}$$

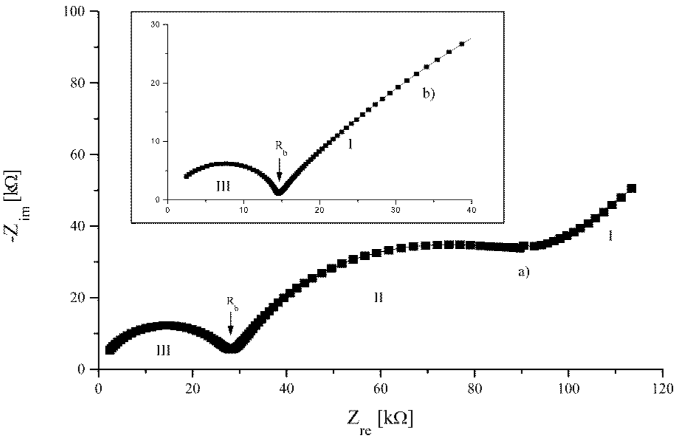

Fig. 1a,b Impedance diagram for undoped YSZ (ZrO_2 + 12 mol% Y_2O_3) in the form of ceramic (a) and as single crystal (b) taken at 397°C (a) and 402°C (b), respectively

The conductivity values were calculated from the analysis of the frequency dependence of *ac* impedance, taking the cell geometry into account and using the electrical equivalent circuit method according to the softwares [9, 10]. The typical behaviour of impedance for the crystalline- as well as ceramic- samples is seen in Fig. 1a,b.

The crystalline samples have no grain boundaries, therefore only electrode and bulk (lattice) resistivity arcs are observed in the impedance diagram; the grain boundary arc is absent. Fig. 1a,b compares the impedance behaviour of single crystal (single grain) and ceramic of ZrO_2 + 12 mol% Y_2O_3 taken at $\sim$ 400°C. The impedance diagram of the single crystal (Fig. 1b) consists of only the electrode (I) and the bulk (III) resistivity arcs as expected. The impedance diagram for the ceramic with an average grain size of the order of 10μm is shown in Fig. 1a. The additional arc (II) in this Figure is present as a result of grain boundaries. As it is possible to see from Fig. 1a,b, the bulk resistivity contributions from the crystalline- and ceramic- samples are very similar in the R_b value. The observed small difference is mainly due to the distribution coefficient of stabilizer Y_2O_3 in ZrO_2 single crystal. The size of the grain boundary arc (II) in the impedance diagram for the ceramic- sample usually varies with the grain size and the impurity content of the sample.

Fig. 2a shows the Arrhenius plots of the electrical conductivity σ for the bulks of undoped ZrO_2 + 12 mol% Y_2O_3 (YSZ) in the crystalline form as well as in the ceramic sample in dependence on the reciprocal temperature ($1/T$). The activation energies E_a estimated according to the general Arrhenius relation

$$\sigma = \sigma_0 \exp -E_a/kT \tag{7}$$

are also noted in this Figure 2a. The dimensions of grain boundary in the ceramic sample are unknown. Therefore the contribution of grain boundaries to the electrical conductivity of the

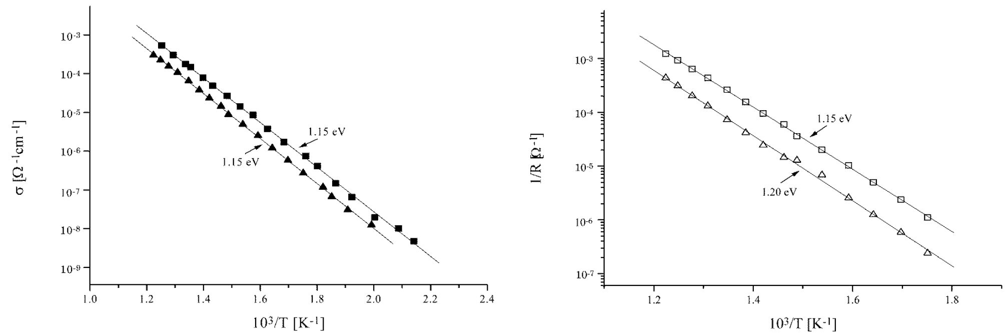

Fig. 2a,b Arrhenius plots of a) bulk conductivity σ for undoped YSZ: ■: single crystal, ▲: ceramic and b) grain boundary resistances for undoped YSZ: □ bulk, △ grain boundary.

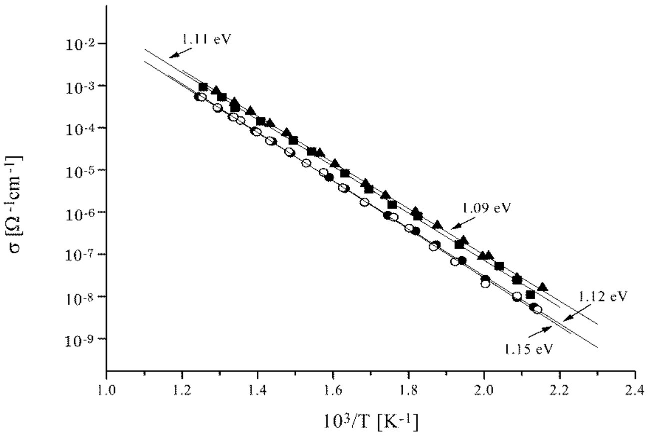

Fig. 3. Arrhenius plots of conductivities σ: ∘ undoped YSZ (reference), • YSZ + Nb_2O_3, (■) YSZ + CuO, (▲) YSZ + Fe_2O_3

sample is plotted only as the dependence of grain boundary resistivity, R_{gb} (determined from the impedance diagram), on the temperature (Fig.2b).

The influence of impurity additions - Nb_2O_3, Fe_2O_3 and CuO - on the charge transport in the crystalline YSZ is shown in the Fig.3. The observed increase of electrical conductivity σ is in agreement with the impurity concentrations dissolved in the YSZ lattice and thereby with the corresponding amount of oxygen vacancies according to the substitutional model proposed in Sec.3.1.

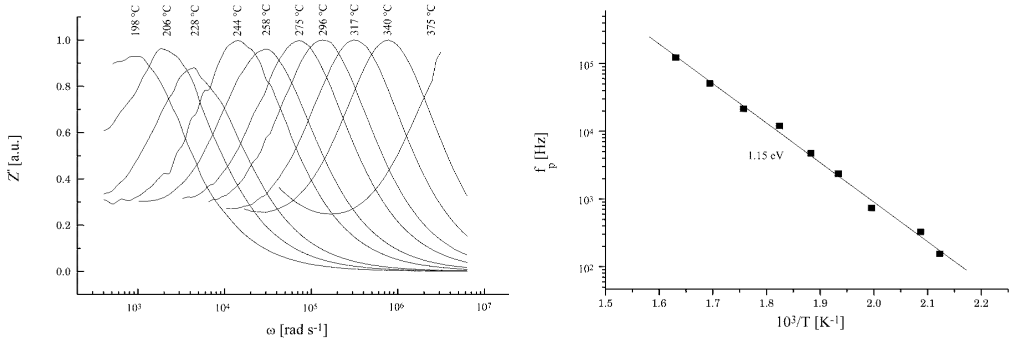

Fig. 4: (a) Imaginary part of impedance Z'' of YSZ + 2.0 wt.% CuO as a function of frequency and temperature (b) Imaginary impedance peak frequency f_p versus reciprocal temperature plots for YSZ + 2.0 wt.% CuO

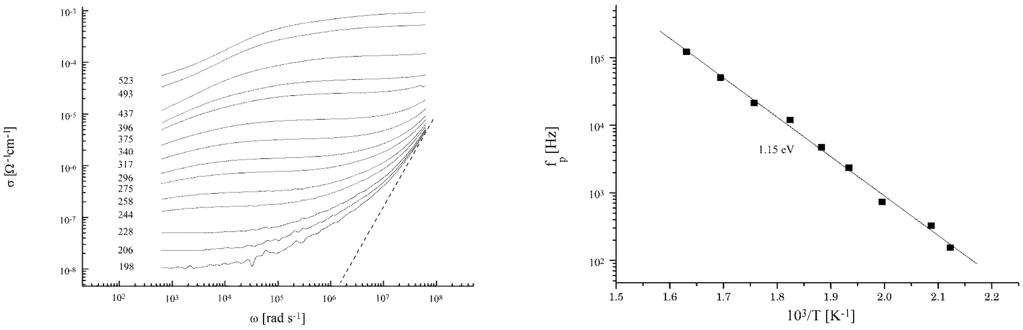

Fig. 5. (a) Variation of conductivity with frequency $\sigma(\omega)$ for YSZ + 2.0 wt.% CuO in the temperature range from 198° to 523°C, (b) Same data as (a) but converted to $\varepsilon''(\omega)$

3.3 Frequency dependence of impedance

The equivalent electrical circuit of a single crystal is usually modelled by a parallel resistance R_p / capacitance C_p combination (see e.g. [11]) so that

$$Z^*(\omega) = Z' + jZ'' = \frac{R_p}{1+\omega^2\tau^2} - j\frac{R_p\omega\tau}{1+\omega^2\tau^2}, \tag{8}$$

where ω is the angular frequency ($\omega = 2\pi f$). The time constant τ is given by the relation

$$\tau = R_p C_p = \varepsilon_0\varepsilon_r/\sigma \tag{9}$$

where ε_0 is the permittivity of free space, 8.854×10^{-14} F cm^{-1}, ε_r is the relative dielectric permittivity of the material and σ is its electrical conductivity. τ characterizes the decay of the

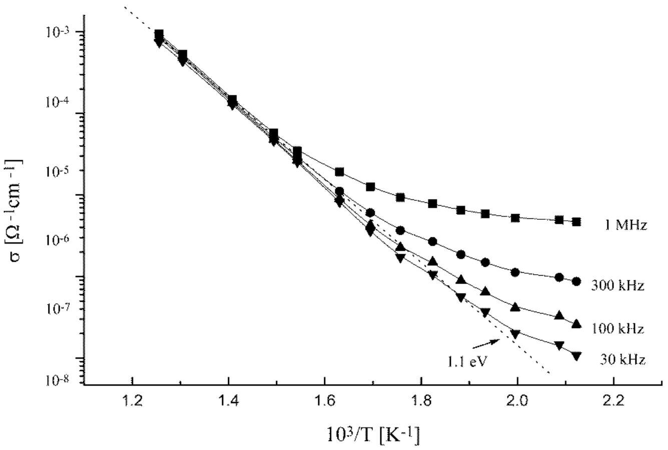

Fig. 6. Variation of electrical conductivity σ with temperature for YSZ + 2.0 wt.% CuO in the frequency range from 30 kHZ to 1 MHz

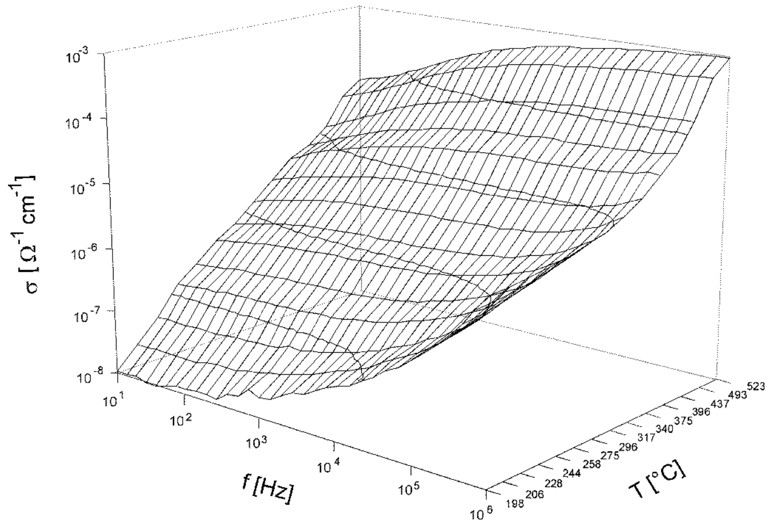

Fig. 7. Combined frequency and temperature dependence of conductivity for YSZ + 2.0 wt.% CuO shown in a 3 - dimensional plot with the contour lines σ = const.

electrical field via the conduction process in the conductor. Therefore the characteristic time constant (relaxation time) τ is determined by fundamental material properties, i.e. the electrical conductivity and the dielectric permittivity.

The imaginary part of the impedance Z'' exhibits a maximum at $\omega_p = \tau^{-1}$. The Z'' versus $\log \omega$ plots for YSZ + 2.0 wt.% CuO are shown in Fig. 4a. The plots, which are normalized to be

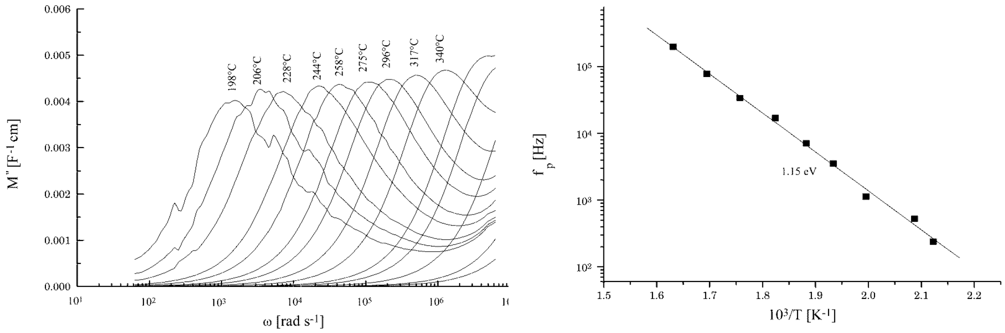

Fig. 8. (a) Imaginary part of electric modulus M'' of YSZ + 2.0 wt.% CuO as a function of frequency and temperature, (b) Imaginary electric modulus peak frequency f_p versus reciprocal temperature plots for YSZ + 2.0 wt.% CuO

comparable, exhibit maxima; the peak frequencies f_p shift towards higher values with increasing temperature. A plot of $\log f_p$ versus $10^3/T$ shows Arrhenius behaviour (Fig. 4b). From the shifts in Fig. 4b is possible to obtain a relaxation time τ_p in the Arrhenius form

$$\tau_p = \tau_0 \exp E/kT$$

with the activation energy E = 1.15 eV and $\tau_0 \sim 10^{-15}$ s, suggesting that it is controlled by a specific ionic hopping process.

3.4 Frequency dependence of electrical conductivity and dielectric permittivity

The frequency dependence of admittance $Y^* = 1/Z^*$ can be derived from eq. (8) as follows:

$$Y^* = Y' + jY'' = 1/R_p + j\omega\tau/R_p \tag{10}$$

The real part of admittance Y' is proportional to the electrical conductivity $\sigma(\omega)$ of the investigated material

$$\sigma(\omega) = KY' = K/R_p, \qquad K = l/A. \tag{11}$$

where K is the cell (geometrical) constant [cm^{-1}], l is the thickness of the sample and A is the electrode area.

The complex relative dielectric permittivity ε_r^* can be derived from the relation

$$Y^* = j\omega\varepsilon_r^* C_0, \qquad C_0 = \varepsilon_0/K, \tag{12}$$

where C_0 is the vacuum capacitance of the cell. Using eq. (10), the frequency dependence of ε_r^* can be obtained as follows:

$$\varepsilon_r^*(\omega) = \varepsilon_r' - j\varepsilon_r'' = \frac{\tau}{R_p C_0} - j\frac{1}{R_p C_0 \omega} = \frac{C_p}{C_0} - j\frac{\sigma}{\varepsilon_0 \omega} \tag{13}$$

Fig. 5a shows the frequency dependence of electrical conductivity, $\sigma(\omega)$, for a YSZ + 2.0 wt.% CuO. It is known that in the low temperature / high frequency region, the addition to the low frequency or "dc" value conductivity obeys a power-law dependence on the frequency of the form

$$\sigma(\omega) = \sigma(0) + B\omega^s \tag{14}$$

in which the exponent $s \sim 1$. According to Jonscher [12], eq.(14) has a general validity for widely different classes of materials ("universal dynamic response"). While the dc conductivity is related to classical ionic transport under the influence of an applied electric field, the frequency dependent term has been attributed to collective effects in which each hopping ion has strong interactions (usually of the Coulombic type) with the surrounding ions (e.g. [13]). This behaviour shows Arrhenius-type temperature dependence. In addition, at low temperatures and/or high frequencies, there is a region of behaviour where $\sigma(\omega)$ is nearly proportional to ω, i.e. $s \cong 1$ in eq. (14). Since $\sigma(\omega) \propto \omega$ (Fig. 5a),

$$\varepsilon_r^*(\omega) = \sigma(\omega)/\varepsilon_0\omega = \text{const.}$$

Fig. 5a shows an example of a set of $\sigma(\omega)$ curves for YSZ + 2.0 wt.% CuO over a wide range of temperatures, while Fig. 5b shows the same data expressed as $\varepsilon''(\omega)$. It is clear that in the low temperature/high frequency range $\sigma(\omega)$ is nearly proportional to ω (the dashed line in Fig 5a) and $\varepsilon''(\omega)$ is approaching to the constant value. The change with temperature is very weak under these conditions.The central parts of both Figs. 5a, 5b correspond to the region, where $\sigma(\omega)$ is nearly constant, i.e. $\varepsilon_r''(\omega) \sim 1/\omega$. The low frequency/high temperature parts of both Figs. 5a, 5b are influenced by the blocking effect of electrodes. The temperature dependence of electrical conductivity $\sigma(\omega)$ for YSZ + 2.0 wt.% CuO for various high frequencies together with the extrapolated conductivity $\sigma(0)$ is possible to see in Fig.6. The combined frequency and temperature dependence of the conductivity for YSZ + 2.0 wt.% CuO shown in a 3-dimensional plot can be seen in Fig.7.

3.5 Frequency dependence of electrical modulus

The electrical modulus formalism was first used to analyse the electrical relaxation in glasses and melts [14,15]. The extension of the modulus treatment to crystalline systems was performed by Hodge et al. [16].

The complex electric modulus M^* is defined as the reciprocal of the complex dielectric permittivity ε_r^*:

$$M^* = \frac{1}{\varepsilon_r^*} = \frac{1}{\varepsilon_r' - j\varepsilon_r''} = \omega C_0 Z'' + j\omega C_0 Z' = M' + jM''. \tag{15}$$

Using eq.(8), the frequency dependence of the complex electrical modulus M^* can be written as

$$M^*(\omega) = (C_0/C_p)\frac{\omega^2\tau^2}{1+\omega^2\tau^2} + \frac{j(C_0/C_p)\omega\tau}{1+\omega^2\tau^2}.$$

The M'' versus $\log\omega$ plots exhibit the analogous maxima (Fig. 8a) as it was possible to observe in the case of Z'' versus $\log\omega$ plots and also with the practically identical values of

E and τ_0 (Fig. 8b). The observed increase of M'' peak heights with increasing temperature is in agreement with the known fact that the number of mobile oxygen vacancies $V_O^{\cdot\cdot}$ increases with increasing temperature. The same behaviour was observed for all investigated doped YSZ compositions.

The behaviour of $\log\sigma$ (calculated from the impedance diagram) versus $10^3/T$ (Fig. 3) has the same Arrhenius character. The activation energies E calculated from the f_p and σ plots are identical within the experimental error. The comparison of electrical conductivity and modulus experimental results suggest that the imaginary electrical modulus M'' peak is the result of the oxygen vacancy $V_O^{\cdot\cdot}$ movement.

4 Conclusions

The utilization of various mechanisms of electrical response for the investigation of crystalline yttria stabilized zirconia doped with Fe_2O_3, Nb_2O_3 and CuO has shown that

- all investigated systems exhibit fcc fluorite structure with a slight change of lattice parameter in dependence on the addition of dopants
- the proposed substitutional model of solid solutions for all investigated systems is in a good agreement with the investigated characteristics
- the conclusions about the studied electrical characteristics are practically the same.

Acknowledgement The work was partially supported by the research grants No. 2 / 5081 / 98 and 1 / 4253 / 97 of the Slovak Grant Agency.

References

[1] J.R. Mac Donald: *MRC, Symp.Proc.* **411** (1996) 71
[2] N. Hirose, A.R. West: *J. Amer. Ceram. Soc.* **79** (1996) 1633
[3] V.I. Aleksandrov, V.V. Osiko, A.M. Prochorov, V.M. Tatarintsev: *Uspechi Khimii* **47** (1978) 385
[4] M. Hartmanova, L. Machovic, A. Koller, F. Hanic, B. Misanik: *Solid State Ionics* **14** (1984) 93
[5] H.E. Swanson, H.F. Mc Murdie, M.C. Morris, E.H. Evans: in *Standards (U.S.) Monograph 25, sec. 4* (1966), 83.
[6] R.D. Shannon: *Acta Crystallogr.* **A32** (1976) 751
[7] V. Saly, S. Chromik: *J. Mater. Sci. Letters* **12** (1993) 1306
[8] J.E. Bauerle: *J. Phys. Chem. Solids* **30** (1969) 2657
[9] B.A. Boukamp: *Equivalent circuit (EQUIVCRT.PAS) users manual.* University of Twente, Department of Chemical Technology, The Netherlands 1989.
[10] J.R. Mac Donald: *CNLS Program LEVM 7.0 Version Software*, 1997.
[11] P. Sarkar, P.S. Nicholson: *Solid State Ionics* **21** (1986) 49
[12] A.K. Jonscher: *Dielectric Relaxation in Solids.* Chelsea Dielectric Press , London 1983 (New Corrected Impression, 1996).
[13] J.C. Dyre: *J. Appl. Phys.* **64** (1988) 2456
[14] J.H. Ambrus, C.T. Moynihan, P.B. Macedo: *J. Phys. Chem.* **76** (1972) 3287
[15] P.B. Macedo, C.T. Moynihan, R. Bose: *Phys. Chem. Glasses* **13** (1972) 171
[16] I.M. Hodge, M.D. Ingram, A.R. West: *Electroanal. Chem. & Interfac.Electrochem.* **58** (1975) 429